

# Disordered magnetism in superconducting $\text{KFe}_2\text{As}_2$ single crystals

V. Grinenko <sup>1</sup>, S.-L. Drechsler <sup>\*,1</sup>, M. Abdel-Hafiez <sup>1</sup>, S. Aswartham <sup>1</sup>, A.U.B. Wolter <sup>1</sup>, S. Wurmehl <sup>1</sup>, C. Hess <sup>1</sup>, K. Nenkov <sup>1</sup>, G. Fuchs <sup>1</sup>, D. Efremov <sup>1</sup>, B. Holzapfel <sup>1</sup>, J. van den Brink <sup>1</sup>, B. Büchner <sup>1,2</sup>

<sup>1</sup> IFW Dresden, D-01171 Dresden, Germany

<sup>2</sup> Technische Universität Dresden, Institut für Festkörperphysik, Germany

Received XXXX, revised XXXX, accepted XXXX

Published online XXXX

**Key words:** superconductivity, pnictides, spin-glass, Griffiths phase

\* Corresponding author: e-mail s.l.drechsler@ifw-dresden.de, Phone: +49-351-4659-384, Fax: +49-351-4659-380

High-quality  $\text{KFe}_2\text{As}_2$  (K122) single crystals synthesized by different techniques have been studied by magnetization and specific heat (SH) measurements. The adopted phenomenological analysis of the normal state properties shows that there are two types of samples both affected by disordered magnetic phases: (i) cluster-glass (CG) like or (ii) Griffiths phase (G) like. For (i) at low applied magnetic fields the  $T$ -dependence of the zero field cooled (ZFC) linear susceptibility ( $\chi_l$ ) exhibits an anomaly with an irreversible behavior in ZFC and field cooled (FC) data. This anomaly is related to the freezing temperature  $T_f$  of a CG. For the investigated samples the extrapolated  $T_f$  to  $B = 0$  varies between 50 K and 90 K. Below  $T_f$  we observed a magnetic hysteresis in the field dependence of the isothermal magnetization ( $M(B)$ ). The frequency shift of the freezing temperature  $\delta T_f = \Delta T_f / [T_f \Delta(\ln \nu)] \sim 0.05$  has an intermediate value, which provides evidence for the formation of a

CG-like state in the K122 samples of type (i). The frequency dependence of their  $T_f$  follows a conventional power-law divergence of critical slowing down  $\tau = \tau_0 [T_f(\nu)/T_f(0) - 1]^{-z\nu'}$  with the critical exponent  $z\nu' = 10(2)$  and a relatively long characteristic time constant  $\tau_0 = 6.9 \cdot 10^{-11}$  s also supporting a CG behavior. The large value of the Sommerfeld coefficient obtained from SH measurements of these samples was related to magnetic contribution from a CG. Samples from (ii) did not show a hysteresis behavior for  $\chi_l(T)$  and  $M(B)$ . Below some crossover temperature  $T^* \sim 40$  K a power-law dependence in the  $\chi_l \propto T^{\lambda_G - 1}$ , with a non-universal  $\lambda_G$  was observed, suggesting a quantum G-like behavior. In this case  $\chi_l$  and  $M(B)$  can be scaled using the scaling function  $M_s(T, B) = B^{1-\lambda_G} Y(\mu B/k_b T)$  with the scaling moment  $\mu \sim 3.5\mu_b$ . The same non-universal exponent was found also in SH measurements, where the magnetic contribution  $C/T \propto T^{\lambda_G - 1}$ .

Copyright line will be provided by the publisher

**1 Introduction** The interplay between superconductivity (SC) and magnetism, and the role of correlation effects in Fe-pnictides are under debate [1,2,3]. It is commonly assumed that in most of the so-called stoichiometric parent compounds nesting between electron (el) and hole (h) Fermi surfaces is responsible for the presence of long-range spin density waves (SDW). To get SC, the SDW should be suppressed by chemical doping or external pressure [1,2]. Therefore, it is believed that SC is driven at least partially by AFM spin fluctuations (sf). In contrast, in some

other of Fe-pnictides such as  $\text{LiFeAs}$  (111) or  $\text{KFe}_2\text{As}_2$  (K122) there is no nesting. Therefore, the role of magnetism in the SC pairing of these compounds is less obvious but it is still believed that remaining sf as in Ba122 [4] or a new type [5] sf can be responsible for SC.

In this paper we demonstrate that the physical properties of clean K122 single crystals are strongly affected by an unexpected glassy like magnetic behavior such as spin-glass (SG) and Griffiths (G) type. It is known that a SG phase gives a nearly linear magnetic contribution to

Copyright line will be provided by the publisher

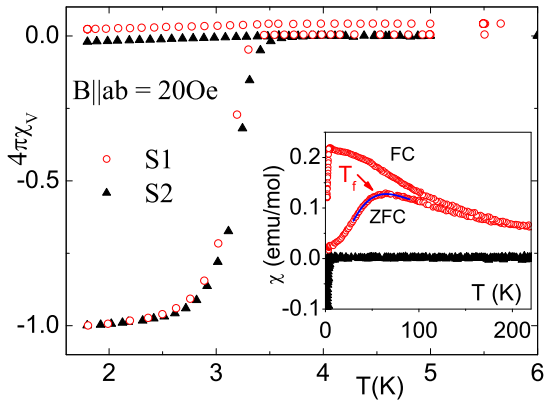


**Figure 1** (Color online) The temperature dependence of the volume susceptibility of S1 and S2 in the SC state. Inset: Their molar susceptibilities in the normal state.

the SH below the freezing temperature  $T_f$  [6,7]. In some cases the SG contribution can be hardly distinguished from the usual electronic (Sommerfeld) contribution to the SH, since it has the same linear  $T$ -dependence and only a weak maximum slightly above  $T_f$ . Therefore, the Sommerfeld coefficient and the deduced strength of correlation effects can be significantly overestimated, if one considers only SH data ignoring thereby the glassy phases. Moreover, the interplay of superconductivity (SC) and *unknown* magnetic phases can lead to confusing conclusions concerning SC gaps [8]. A clear understanding of various coexisting or competing forms of magnetism should be addressed first.

## 2 Experimental results and discussion

### 2.1 Samples

K122 single crystals have been grown using a self-flux method (FeAs-flux (S1) and KAs-flux (S2)). The high quality of the grown single crystals was assessed by complementary techniques. Several samples were examined with a Scanning Electron Microscope (SEM Philips XL 30) equipped with an electron microprobe analyzer for a semi-quantitative elemental analysis using the energy dispersive x-ray (EDX) mode (for details see [9,10]). Resistivity of all measured samples showing a metallic behavior at all  $T$  with a  $\text{RRR}_5 = \rho(300\text{ K})/\rho(5\text{ K}) \approx 400\text{-}500$ , where  $\rho(300\text{ K})$  and  $\rho(5\text{ K})$  is resistivity at  $T = 300$  and  $5\text{ K}$ , respectively, comparable with the best values reported in the literature. The resistivity data will be published elsewhere. Low- $T$  SH and ac susceptibility were determined using a PPMS (Quantum Design). The dc magnetic susceptibility has been measured in a SQUID (Quantum Design) magnetometer. In this paper the data for two representative single crystals are shown.

#### 2.1.1 Magnetization measurements

**Samples with cluster glass behavior** Fig. 1 depicts the  $T$ -dependence of the volume susceptibility ( $\chi_v$ ) determined from dc magnetization of our samples mea-

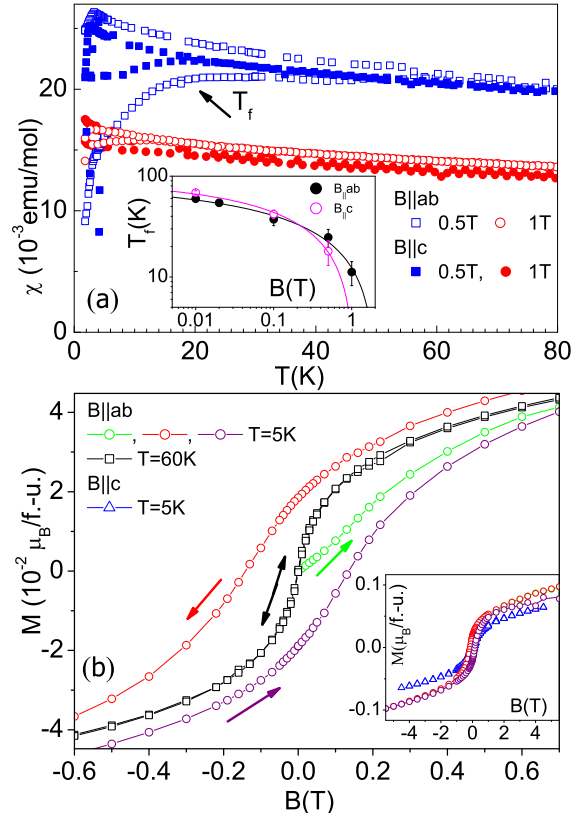


**Figure 2** (Color online) (a) The molar susceptibility  $\chi_l(T) = M/B$  for S1 crystal measured at different magnetic fields  $B$ .  $M$  is the magnetization. Inset: field dependence of freezing temperature for field  $B_{||ab}$  and  $B_{||c}$ . (b) Field dependence of magnetization of S1 crystal measured after ZFC at  $T=5\text{ K}$  and  $T=60\text{ K}$  ( $B_{||ab}$ ). Inset: field dependence of magnetization at  $B_{||ab}$  and  $B_{||c}$  and  $T=5\text{ K}$ .

sured under both zero-field-cooled (ZFC) and field-cooled (FC) conditions with the field  $B_{||ab} = 20\text{ Oe}$ . Bulk SC of our samples is confirmed by 'full' diamagnetic signals of the ZFC data at low  $T$ . For sample S1, a clear splitting between ZFC and FC normal state linear susceptibility  $\chi_l(T) = M(T)/B$  curves is observed below  $100\text{ K}$  (see the inset of Fig. 1), where  $M(T)$  is a magnetization in the field  $B$ . The maximum in the ZFC  $\chi_l(T)$  is attributed to the freezing temperature of a spin glass (SG) type phase at  $T_f \approx 65\text{ K}$  and  $B = 20\text{ Oe}$  [11].  $T_f$  decreases with increasing field and at  $5\text{ T}$  no splitting was observed down to  $2\text{ K}$  (see Fig. 2a). The field dependence of  $T_f$  is shown in the inset of Fig. 2a. The extrapolated value of  $T_f(B = 0) \sim 90\text{ K}$  is a relatively high value. This might point to a large concentration of the involved magnetic moments (MM)  $\gtrsim 10\%$  in sample S1 [7]. Such a high value of MM is expected from entropy estimations, too (see section 2.2). On the other hand, structural investigations did not reveal any impurity phase (see section 2.3). Therefore, we speculate that the high value of  $T_f$  might be

caused by a low-lying excited incommensurate spin density wave state [12]. For a more detailed consideration of this scenario see Ref. 13. In addition, an upshift of the maximum and its lowering with increasing frequency  $\nu$  of the ac susceptibility, generic for a SG ordering [6,7] (Fig. 3), was observed for crystal S1. The value of the frequency shift of  $T_f$  [11]:

$$\delta T_f = \frac{\Delta T_f}{[T_f \Delta(\log \nu)]} \sim 0.05. \quad (1)$$

is above the range 0.001-0.02 expected for canonical SG but well below  $\sim 0.3$  observed in the case of superparamagnets [7]. Such an intermediate value of the frequency shift is usually related to a the so-called cluster glass (CG) behavior [14,15]. The frequency dependence of the  $T_f$  shown in inset Fig. 3 follows a conventional power-law divergence of critical slowing down [7, 15]:

$$\tau = \tau_0 \left[ \frac{T_f(\nu)}{T_f(0)} - 1 \right]^{-z\nu'}, \quad (2)$$

where  $\tau = 1/\nu$  is the relaxation time corresponding to the measured frequency  $\nu$ ,  $\tau_0$  is the characteristic relaxation time of single spin flip,  $T_f(\nu = 0, B = 50e) \approx 71$  K is the spin-glass temperature as the frequency tends to zero adopted from dc susceptibility measurements (inset Fig. 2a), and  $z\nu'$  is the dynamic critical exponent. It is convenient to rewrite Eq. 2 in the form:

$$\ln(\tau) = \ln(\tau_0) - z\nu' \ln(t), \quad (3)$$

where  $t = T_f(\nu)/T_f(0) - 1$ . The fit of the experimental data by a power-law divergence Eq. 3 is shown in the inset Fig. 3. The best fit was obtained with  $z\nu' = 10(2)$  and  $\tau_0 = 6.9 \cdot 10^{-11}$ s. The value of  $z\nu'$  is in the range of 4 to 12 observed for typical SG [15]. On the other hand the value of  $\tau_0$  is large as compared to  $10^{-12} - 10^{-14}$ s observed for structureless SG systems, which is of the order of the spin-flip time of atomic magnetic moments ( $10^{-13}$ s) [16]. This suggests a slow spin dynamics in our crystal S1, likely due to the presence of interacting clusters rather than individual spins.

Another signature of a SG-like behavior for crystal S1 is a hysteresis in the magnetization data below  $T_f$  with a reduced ZFC susceptibility at low fields (Fig. 2b). This behavior is expected in the case of SG or CG systems [7, 14, 17] below  $T_f$  and also excludes superparamagnetic behavior in our samples where no hysteresis was observed [18]. On the other hand, in the case of canted antiferromagnetic (AF) or ferromagnetic (FM) impurity phases hysteresis is expected but with a higher susceptibility at low fields because the clusters are at first saturated along their local easy axis, and only after that various clusters become fully aligned along the applied field [16]. Therefore, our  $M(B)$  data exclude (large) clusters of impurity phases such as FeAs, Fe<sub>2</sub>As or other iron compounds. The same conclusion can be drawn from our SH measurements (see below).

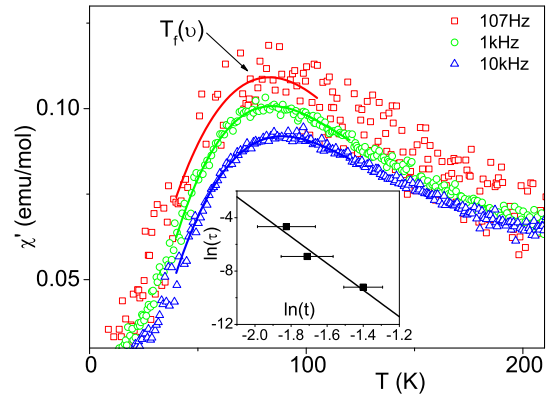


**Figure 3** (Color online)  $T$ -dependence of the real part of the ac susceptibility for sample S1 measured for three different frequencies  $\nu$  at 5 Oe ac field amplitude. Inset: the  $\nu$ -dependence of the freezing temperature plotted as  $\ln(\tau)$  vs.  $\ln(t)$ , where  $t$  denotes the reduced temperature  $t = T_f(\nu)/T_f(0) - 1$ .

We also observed the displacement of the ZFC magnetization compared to magnetization after complete hysteresis loop at magnetic field applied parallel to  $ab$  plane (inset Fig. 2b). For the field along the  $c$ -axis no displacement was observed. This indicates that the glassy behavior is dominated by a magnetic interaction between moments lying in the  $ab$ -plane.

**Samples with Griffiths-phase behavior** In contrast, the  $T$ -dependence of the linear susceptibility  $\chi_l(T)$  of some crystals S2 does not show a difference between ZFC and FC curves above  $T_c$ . The  $\chi_l(T)$  data of one of the S2 crystals is shown in Fig. 4a. At high  $T > 200$  K,  $\chi_l(T)$  follows a Curie-Weiss behavior with an AFM  $\Theta_c = -117$  K [19]. At  $T \lesssim 120$  K  $\chi_l(T)$  shows a plateau-like feature with a field independent susceptibility above  $B = 1$  T. In a view of the observed CG in sample S1, we relate this flattening to a tendency to form magnetic clusters in the crystals S2, too. However, with lowering  $T$  after a weak reduction of  $\chi_l(T)$  instead to form a CG phase in crystal S2, below  $T^*$  an exponential increase of the susceptibility is observed:

$$\chi_l(T) = \chi_{l0} + \frac{Cu_G}{T^{1-\lambda_G}}, \quad (4)$$

where  $\chi_{l0}$  is a  $T$ -independent susceptibility, and  $Cu_G$  is a background constant. A power-law with the exponent  $\lambda_G$  was found up to the highest measured field 7 T (see Fig. 4a). This exponential behavior is quite similar to the reported one for the weak itinerant ferromagnetic alloy Ni<sub>1-x</sub>V<sub>x</sub> [20], where the formation of a Griffiths (G) phase with a non-universal exponent was observed near a FM quantum critical point. Following the analysis proposed there, the field and  $T$ -dependence of the magnetization can

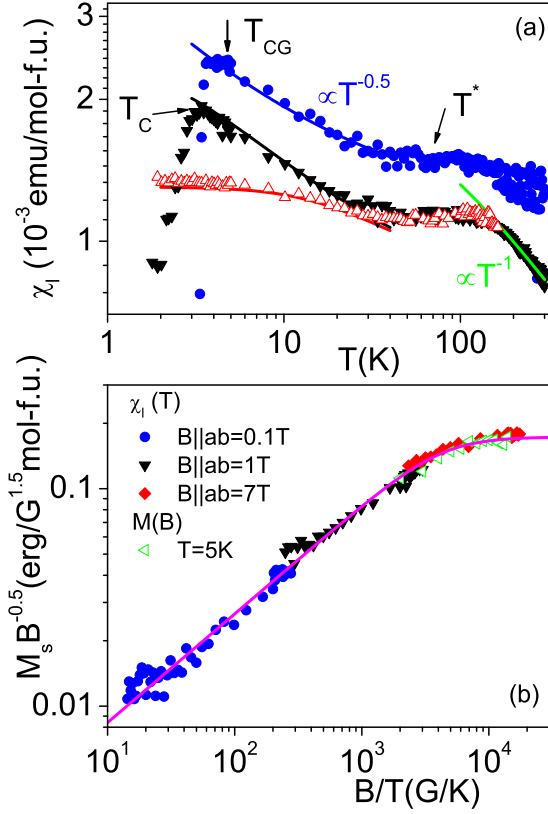


**Figure 4** (Color online) (a) The molar susceptibility  $\chi_l(T) = M/B$  for crystal S2 measured in different magnetic fields  $B$ , where  $M$  is the magnetization. Fitting curves using Eq. 5. (b) The scaled magnetization  $M_s B^{-0.5} = (M(T, B) - \chi_{l0} B) B^{-0.5}$  vs.  $B/T$  for crystal S2. (see Eq. 5)

be scaled on a single curve Fig. 4b:

$$M_s(T, B) = B^{1-\lambda_G} Y\left(\frac{\mu B}{k_b T}\right), \quad (5)$$

where  $\mu$  is the scaling moment and  $Y = A'/(1+z^{-2})^{\lambda_G/2}$  a scaling function with  $A' = A/\mu^{\lambda_G}$  as a constant. To scale the data using Eq. 5 we have subtracted the  $T$ -independent susceptibility  $\chi_{l0}$  from  $\chi_l(T)$  and  $\chi_{l0} B$  from  $M(H)$ , correspondingly. For sample S2 (Fig. 4) a scaling was observed for  $\lambda_G \approx 0.5(1)$  with a scaling moment  $\mu \sim 3.5\mu_b$ . According to Ref. 20 the obtained moment can be related to a typical cluster size in crystal S2. The SH data are also in agreement with the G-like scenario (see below). Therefore, we ascribe the anomalous power-law of  $\chi(T)$  at low  $T < T^* \approx 50$  K to the formation of a quantum G-phase.

## 2.2 Specific heat measurements

**Specific heat in the normal state** We have found that the glassy magnetic subsystems (observed in the magnetization measurements) do also contribute to the SH shown in Fig. 5a. In case of SG or CG phases the mag-

netic contribution  $C_{CG}$  to the SH varies almost linearly at  $T < T_f$  like the usual electronic contribution in case of a FL [7,6,21,22]. Empirically, this behavior can be approximated by

$$C_{CG} \approx \gamma_{CG} T + \varepsilon_{CG2} T^2, \quad (6)$$

or

$$C_{CG} \approx \varepsilon_{CG1.5} T^{1.5}, \quad (7)$$

where  $\gamma_{CG}$ ,  $\varepsilon_{CG2}$  and  $\varepsilon_{CG1.5}$  are CG constants. The  $\varepsilon_{CG1.5}$  contribution can be interpreted as originating from short-range 3D ferromagnetic (FM) spin waves which can exist in a FM clusters [23], also a linear contribution to SH can be expected for 2D FM spin waves. Then, the normal state SH of sample S1 reads

$$C_p^{S1}(T) = \gamma_{el} T + C_m^{CG} + \beta_3 T^3 + \beta_5 T^5, \quad (8)$$

where  $C_m^{CG}$  is given by Eq. 6 and Eq. 7,  $\gamma_{el}$  is an intrinsic electronic contribution and  $\beta_3, \beta_5$  are a lattice contribution. In case of a G-phase (sample S2),  $C(T)_G/T \propto \chi(T)$  is expected [24,25]. Hence, for the SH we have:

$$C_p(T)^{S2} = \gamma_{el} T + \gamma_G T^{\lambda_G} + \beta_3 T^3 + \beta_5 T^5, \quad (9)$$

where  $\lambda_G \approx 0.5(1)$  according to our magnetization data. To reduce the number of fitting parameters in Eqs. 8 and 9, we analyzed the difference:

$$[C_p^{S1}(T) - C_p^{S2}(T)]/T = C_{CG}^{S1} - \gamma_G T^{\lambda_G - 1}. \quad (10)$$

This allow us to exclude the lattice contributions  $\beta_3, \beta_5$ , as well as the linear electronic term  $\gamma_{el}$  which are all supposed to be nearly the same for both crystals, respectively. The fit of the experimental data by Eq. 10 is shown in Fig. 5b. i) In the case of Eq. 6 it gives:  $\gamma_{CG}^{S1} = 36$  mJ/mol·K<sup>2</sup>,  $\varepsilon_{CG2} = 2.0$  mJ/mol·K<sup>3</sup> and  $\gamma_G = 104$  mJ/mol·K<sup>1.5</sup>, respectively. Then, using in Eq. 9 obtained magnetic contribution we have estimated the *intrinsic*  $\gamma_{el}^i \approx 52$  mJ/mol·K<sup>2</sup> for sample S2 with the lattice terms  $\beta_3^i = 0.59$  mJ/mol·K<sup>4</sup> and  $\beta_5^i = 1.20 \cdot 10^{-3}$  mJ/mol·K<sup>6</sup>, respectively. The obtained  $\beta_3^i$  corresponds to a Debye temperature  $\Theta_D^i \approx 254$  K. ii) In the case of validity of Eq. 7 it gives:  $\varepsilon_{CG1.5} = 14.9$  mJ/mol·K<sup>3</sup> and  $\gamma_G = 75.3$  mJ/mol·K<sup>1.5</sup>, respectively. Then the *intrinsic*  $\gamma_{el}^{ii} \approx 68$  mJ/mol·K<sup>2</sup> is the same for S1 and S2 crystals with slightly different lattice terms as compared to those obtained in the analysis (ii):  $\beta_3^{ii} = 0.46$  mJ/mol·K<sup>4</sup> and  $\beta_5^{ii} = 1.86 \cdot 10^{-3}$  mJ/mol·K<sup>6</sup>, respectively. This value of  $\beta_3^{ii}$  corresponds to a Debye temperature  $\Theta_D^{ii} \approx 276$  K. Both analysis give reasonable values of the lattice contribution (for example, in the case of  $\text{Ba}_{0.68}\text{K}_{0.32}\text{Fe}_2\text{As}_2$  a Debye temperature of 277K was estimated [26]) and essentially reduced  $\gamma_{el} \approx 52 - 68$  mJ/mol·K<sup>2</sup> as compared to nominal values  $\gamma_n \approx 100$  mJ/mol·K<sup>2</sup> [27,8] obtained with out accounting for magnetic contributions. The SH data at  $B = 9$  T shown in Fig. 5a can be considered as a support



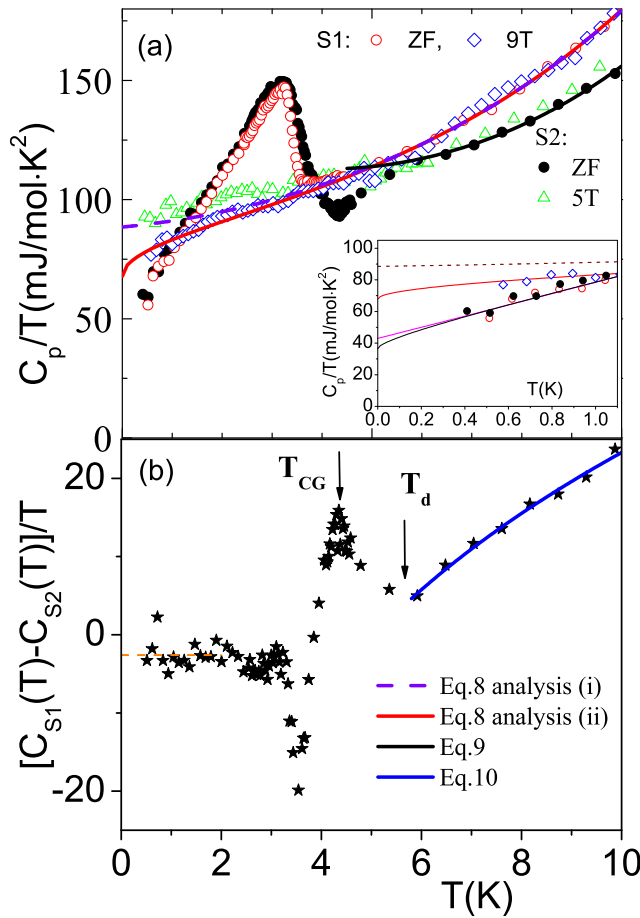


**Figure 5** (Color online) (a) The specific heat of our two K122 samples. Inset: low temperature part of the SH at zero field. (b) The plot  $[C_p^{S1}(T) - C_p^{S2}(T)]/T$ .

of analysis (ii), since this analysis provides essentially a better agreement between the experimental data and the fitting curves at low- $T$ . However, we cannot exclude that large field enhances FM order in S1 crystals and actually change the entropy of SG at low temperatures.

Below  $T_d \sim 6$  K the data for S2 deviate from the fit-curve (Fig. 5). At  $T_{CG} \sim 4$  K, slightly above  $T_c$ , (see Fig. 5a) another magnetic anomaly is well visible in the SH data. Additionally, slightly above  $T_{CG}$  we observed a plateau-like feature in  $\chi(T)$  at relatively low fields (see Fig. 4a). We ascribe  $T_d$  to the freezing of large cluster dynamics in accord with the behavior expected for a quantum G-phase (see Ref. [28]) followed by the final formation of a CG phase due to the RKKY interaction between the clusters at  $T_{CG}$  in crystal S2, too (for an illustration see also Fig. 6).

**Specific heat in the superconducting state** Measurements in SC state have shown that there is a large residual Sommerfeld coefficient observed for all investigated

samples (see inset Fig. 5a). The fit below 1K gives a residual contribution for crystal S1  $\gamma_{res1}^{S1} \approx 43$  mJ/mol·K<sup>2</sup> and about  $\gamma_{res1}^{S2} \approx 46$  mJ/mol·K<sup>2</sup> for S2 [29]. The  $\gamma_{res1}^{S1}$  is close to  $\gamma_{CG}^{S1} = 36$  mJ/mol·K<sup>2</sup> estimated for the normal state using analysis (i). The closeness of these values would indicate that  $\gamma_{SG}^{S1}$  is weakly effected by the SC transition and also excludes essentially a non-superconducting volume fraction for our the samples. The latter is also supported by the large absolute value of the SH jump at  $T_c$  compared to the reported in the literature values [8,27]. In the case of [8] it was observed that  $C_p/T$  of the investigated crystals tends to zero at  $T = 0$  after AFM type magnetic transition at  $T \sim 0.7$ K. This demonstrates that almost all itinerant quasi-particles are gapped at  $T = 0$ . Therefore, we conclude that the large residual  $\gamma_{res}$  in the SC state of our samples is mainly due to the magnetic contribution from a CG. On the other hand, using  $\epsilon_{CG1.5} = 14.9$  mJ/mol·K<sup>3</sup> from analysis (ii), we get  $\gamma_{res2}^{S1} \approx 36$  mJ/mol·K<sup>2</sup>. This value is nearly a half of  $\gamma_{el}^{ii} \approx 68$  mJ/mol·K<sup>2</sup>. In contrast to the conclusion obtained from analysis (i), it would mean that the CG phase in SC state is different from the CG in the normal state, since we exclude a large non-SC part of our samples. This can be possible, since itinerant electrons responsible for the RKKY interaction are affected by the SC transition. Thus, on this stage we cannot decide which analysis (i) or (ii) is more sophisticated. Therefore, we estimate the *intrinsic*  $\gamma_{el}^{ii} \approx 52 - 68$  mJ/mol·K<sup>2</sup>. A more detailed report of the superconducting properties including microscopic considerations will be given elsewhere.

**2.3 Possible disorder induced quantum phase transitions** Up to now the structural investigation of the cleaved surface of the samples such as EDX, XRD and SEM did not reveal any secondary phases [9,10].

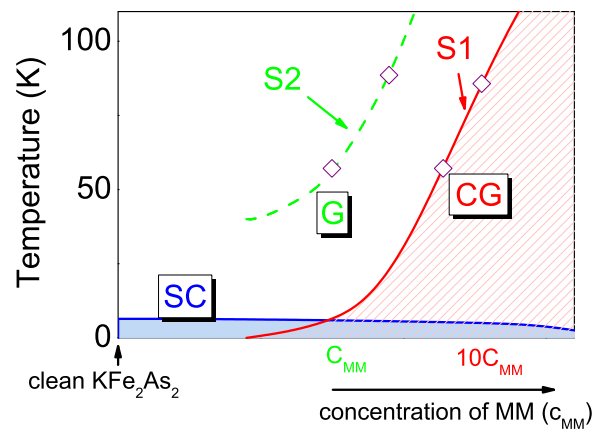


**Figure 6** (Color online) Schematic phase diagram of extrinsic magnetic moments (MM) driven quantum phase transitions. Notation of phases: SC - superconductivity, G - Griffiths, CG - cluster glass, S1, S2 - samples from this work.

Therefore, we enforced to adopt a 'point'-defect model such as vacancies or interstitials of Fe atoms. To compare the amount of magnetic clusters contributing to a glassy phases of our samples, we calculated the magnetic entropy  $S_m = \int (C_m/T) dT$  using the obtained above magnetic contributions.  $S_m^{S2}$  for crystal S2 related to CG and G phases between 0 and  $T^* \approx 50$  K (where the quantum Griffiths behavior appears in the magnetization data Fig. 4a) is  $\sim 0.074 \text{RJ/mol-Fe}\cdot\text{K}^2$ . The estimate for crystal S2 related to the CG phases below  $T_f \approx 87$  K gives an essentially higher value than  $S_m^{S1}$ . In the case of validity of analysis (i)  $\sim 0.64 \text{RJ/mol-Fe}\cdot\text{K}^2$  and for the case of analysis (ii)  $\sim 0.48 \text{RJ/mol-Fe}\cdot\text{K}^2$  for the magnetic contribution have been obtained, respectively. Hence, we conclude that in the normal state crystal S1, it can contain up to 10 times more magnetic clusters than S2 does. Summarizing our experimental observations of disordered magnetic phases in K122, we can propose a quantum phase transition of spin glass type with strong quantum G-phase effects (see Fig. 6) driven by some tuning parameter  $p$  which is responsible for the formation of magnetic moments (MM) in K122. The physical nature of  $p$  should be unraveled in future investigations such as spin and nuclear magnetic resonance and/or Mössbauer spectroscopy. These techniques can be helpful to estimate the amount and the distribution of MM in K122 single crystals.

**3 Conclusions** To summarize, analyzing magnetization and specific heat data, we found out that even in high-quality  $\text{KFe}_2\text{As}_2$  single crystals glassy magnetic behavior like in spin-, cluster-glasses and Griffiths phases may occur near superconductivity and coexist with it. The magnetic contribution is responsible for a large value of the nominal Sommerfeld coefficient  $\gamma_n \sim 100 \text{ mJ/mol}\cdot\text{K}^2$  of this compound. The analysis of the SH data has shown that magnetic contribution amounts up to 50% of  $\gamma_n$ . In this way, the intrinsic value of the Sommerfeld coefficient  $\gamma_{el} \approx 52 - 68 \text{ mJ/mol}\cdot\text{K}^2$  was estimated. We observed that various samples exhibit different disordered magnetic contributions depending on the amount and distribution of magnetic moments (MM). This suggests an extrinsic origin of MM which can be caused by point defects such as vacancies or Fe interstitials. Therefore, we proposed a scenario of disorder induced spin glass type quantum phase transitions accomplished by strong quantum Griffiths effects. Further investigations are required to elucidate the physical origin and the distribution of such MM.

**Acknowledgements** We thank J.A. Mydosh, U. Rößler, and D. Evtushinsky for discussions. Our work was supported by the DFG (SPP 1458 and the Grants No. GR3330/2, WU 595/3-1 (S.W.)) as well as the IFW-Pakt für Forschung.

## References

- [1] D. C. Johnston *Advances in Physics* **59**, 803 (2010).
- [2] G. R. Stewart, *Rev. Mod. Phys.* **83**, 1589 (2011).
- [3] Y. Bang *Supercond. Sci. Technol.* **25**, 084002 (2012).

- [4] M. Hirano, Y. Yamada, T. Saito *et al.* *J. Phys. Soc. Jpn.* **81**, 054704 (2012).
- [5] S. W. Zhang, L. Ma, Y. D. Hou *et al.* *Phys. Rev. B* **81**, 012503 (2010).
- [6] K. Binder and A. P. Young, *Rev. Mod. Phys.* **58**, 801 (1986).
- [7] J. A. Mydosh, *Spin glasses: an experimental introduction* (Taylor and Francis, London - Washington, DC, 1993).
- [8] J. S. Kim, E. G. Kim, G. R. Stewart, X. H. Chen, and X. F. Wang, *Phys. Rev. B* **83**, 172502 (2011).
- [9] M. Abdel-Hafiez, S. Aswartham, S. Wurmehl, V. Grinenko, S.-L. Drechsler, A. U. B. Wolter, and B. Büchner *Phys. Rev. B* **85**, 134533 (2012).
- [10] S. Aswartham, S. Wurmehl, and B. Büchner unpublished.
- [11] To define the  $T_f$  by the same criteria, the  $T$ -dependence of the dc and the ac susceptibilities were fitted by a cubic polynomial as shown in Figs. 1-3. Next  $T_f$  was attributed to the maximum calculated from that cubic polynomial.
- [12] A. W. Overhauser, *J. Phys. Chem. Solids* **13** 71 (1960).
- [13] V. Grinenko *et al.*, e-print arXiv:1203.1585.
- [14] N. Marcano, J. C. Gomez Sal, J. I. Espeso, L. Fernandez Barquin, and C. Paulsen, *Phys. Rev. B* **76**, 224419 (2007).
- [15] V. K. Anand, D. T. Adroja, and A. D. Hillier, *Phys. Rev. B* **85**, 014418 (2012).
- [16] A. Malinowski, V. L. Bezusyy, R. Minikayev, P. Dziawa, Y. Syryanyy, and M. Sawicki, *Phys. Rev. B* **84**, 024409 (2011).
- [17] B. R. Coles, B. V. Sarkissian and R. H. Taylor *Phil. Mag. B* **37**, 489 (1978).
- [18] C. P. Bean and J. D. Livingston, *J. Appl. Phys.* **30**, S120 (1959).
- [19] We also observed a Curie-Wiess behavior at high- $T$  for samples with a CG-phase having lower values of  $T_f$  than shown in Fig. 1 and Fig. 2.
- [20] S. Ubaid-Kassis, T. Vojta, and A. Schroeder, *Phys. Rev. Lett.* **104**, 066402 (2010).
- [21] D. G. Dawes and B. R. Coles, *J. Phys. F: Metal Phys.* **9**, L215 (1979).
- [22] D. L. Martin, *Phys. Rev. B* **21**, 1906 (1980).
- [23] J. O. Thomson and J. R. Thompson *J. Phys. F: Metal Phys.* **11**, 247 (1981).
- [24] A. H. Castro Neto, G. Castilla and B. A. Jones *Phys. Rev. Lett.* **81**, 3531 (1998).
- [25] G. R. Stewart, *Rev. Mod. Phys.* **73**, 797 (2001).
- [26] P. Popovich, A. V. Boris, O. V. Dolgov *et al.* *Phys. Rev. Lett.* **105**, 027003 (2010).
- [27] H. Fukazawa, T. Saito, Y. Yamada *et al.* *J. Phys. Soc. Jpn.* **80**, SA118 (2011).
- [28] T. Vojta, *J. Low Temp. Phys.*, **161**, 299 (2010).
- [29] Note that a large value of  $\gamma_{CG}$  is expected in case of SG or CG [7, 21]. In contrast, the magnetic impurity phases (large clusters) would give only a small contribution at low T. For example,  $\text{Fe}_2\text{As}$  has  $\gamma=21.8 \text{ mJ/mol}\cdot\text{K}^2$  [30] and  $\text{FeAs}$  has  $\gamma \approx 6.65 \text{ mJ/mol}\cdot\text{K}^2$  [31], only. Therefore, even a very high contamination by these impurities would provide only several mJ at low T.
- [30] D. A. Zocco, D. Y. Tütün, J. J. Hamlin *et al.* *Supercond. Sci. Technol.* **25**, 084018 (2012).
- [31] D. Gonzalez-Alvarez, F. Gronvold, B. Falk, E. F. Westrum, R. Blachnik, and G. Kudermann, *J. Chem. Thermodynamics* **21**, 363 (1989).